

Conference paper

Irina A. Stenina and Andrey B. Yaroslavtsev*

Nanomaterials for lithium-ion batteries and hydrogen energy

DOI 10.1515/pac-2016-1204

Abstract: Development of alternative energy sources is one of the main trends of modern energy technology. Lithium-ion batteries and fuel cells are the most important among them. The increase in the energy and power density is the essential aspect which determined their future development. We provide a brief review of the state of developments in the field of nanosize electrode materials and electrolytes for lithium-ion batteries and hydrogen energy. The presence of relatively inexpensive and abundant elements, safety and low volume change during the lithium intercalation/deintercalation processes enables the application of lithium iron phosphate and lithium titanate as electrode materials for lithium-ion batteries. At the same time, they exhibit low ionic and electronic conductivity. To overcome this problem the following main approaches have been applied: use of nanosize materials, including nanocomposites, and heterovalent doping. Their impact in the property change is analyzed and discussed. Hybrid membranes containing inorganic nanoparticles enable a significant progress in the fuel cell development. Different approaches to their preparation, the reasons for ion conductivity and selectivity change, as well as the prospects for their application in low-temperature fuel cells are discussed. This review may provide some useful guidelines for development of advanced materials for lithium ion batteries and fuel cells.

Keywords: composite membranes; electrochemistry; electrodes; materials chemistry; membranes; Mendeleev XX; nanocomposites; nanostructured materials.

Introduction

Nowadays, most of the technologies are associated with energy consumption, and technological progress is inevitably accompanied by its steady increase [1, 2]. In the beginning of the 20th century, 70 % of energy was produced from coal, while since the mid 20th century oil became the dominant energy source [3]. Conversion of this type of fuels to energy is associated with enormous emissions of carbon, sulfur and nitrogen oxides, as well as products of incomplete combustion into the atmosphere. With the increase in environmental pollution and the decrease in oil and gas resources, the search for clean and renewable energy sources becomes an actual problem. So, solar and wind energies are of particular interest, due to their high availability, environmental friendliness and safety [4].

Efficiency of the most requested today solar cells is low. Moreover, their time-of-use is strictly limited. The annual solar irradiance in Russia ranges from 800 to 1500 kWh/m². And the average daily insolation in Moscow is 0.33 kWh/m² in December, and 5.6 kWh/m² in June [5]. Energy consumption, however, varies in an

Article note: A collection of invited papers based on presentations at the XX Mendeleev Congress on General and Applied Chemistry (Mendeleev XX), held in Ekaterinburg, Russia, September 25–30 2016.

***Corresponding author: Andrey B. Yaroslavtsev**, Kurnakov Institute of General and Inorganic Chemistry of the Russian Academy of Sciences, 31 Leninsky pr., Moscow 119991, Russia, e-mail: yaroslav@igic.ras.ru

Irina A. Stenina: Kurnakov Institute of General and Inorganic Chemistry of the Russian Academy of Sciences, 31 Leninsky pr., Moscow 119991, Russia

almost opposite way. Similar problems are relevant for wind power generators. All this determines the need for energy storage systems to be applied. Among them, lithium-ion batteries, as well as steam electrolyzer and fuel cell (FC) based systems are generally accepted as the most promising [2]. Due to the high self-discharge, application of lithium-ion batteries cannot compensate for the annual energy fluctuations. However, they are perfectly suitable for short-time energy storage. Another major problem is associated with the power sources for portable devices and wireless electric tools.

At the present time, the lithium-ion batteries having high capacity and good reliability, dominate this market [6, 7], while the fuel cell market has not fully formed yet. Nevertheless, almost 90 % of total sales are provided by low-temperature FCs based on proton exchange membranes [2]. Their efficiency is determined by the properties of both the catalyst and proton exchange membrane [8–10]. Potential difference of lithium intercalation and deintercalation into cathode and anode materials, along with their electrochemical capacity, determine the energy storage capacity of a lithium-ion battery [11–13]. The present review is hence focused on nanoscale cathode and anode materials for lithium-ion batteries, and also on hybrid proton exchange membranes for fuel cells. In accordance with the specifics of this issue, we have focused on the studies carried out by our team.

Electrode materials for lithium ion batteries

Lithium ion batteries (LIBs) have been widely used in portable electronic devices and wireless electric tools. Recently, they have also been recognized in the electric vehicle power sources market due to high energy density and reliability [6]. The electrochemical performance of LIBs depends sensitively on the properties of electrode materials. To ensure high capacity and reliability, the electrode materials should have low molecular weight and be able to insert reversibly a large amount of lithium; they also should not dissolve or react with the solvent and the other electrolyte component, particularly during cycling. Furthermore, the operating potential of an anode material should be close to that of metallic lithium; for the cathode, on the contrary, it should be much more higher [7, 13]. Attention was, hence, drawn to graphite and silicon first. However, the latter shows comparatively low cycling stability, in particular at high charge/discharge rates [14]. Commercial lithium ion battery uses lithium cobalt oxide as cathode material; it can however be charged only to 130–140 mAh/g, due to the instability of its oxidized form [15]. In addition, cobalt utilization is rather expensive and its disposal has introduced an environmental concern [16]. More recently, cathode and anode materials based on lithium iron phosphate and lithium titanate, respectively, have attracted considerable attention. On the one hand, their advantages are low volume change during lithium intercalation [17], good cycling stability, comparatively low cost, and safety. At the same time, low conductivity is a common disadvantage of these materials.

Cathode materials based on lithium iron phosphate

Lithium iron phosphate (LiFePO_4) was first proposed as a cathode material by Goodenough et al. [18]. Lithium deintercalation from LiFePO_4 leads to FePO_4 formation, whereas the mutual solubility of these two phases is only 2 and 4 %, respectively [17]. As a result, only the $\text{LiFePO}_4/\text{FePO}_4$ ratio changes during the charge/discharge, determining potential plateau at about 3.5 V [19].

The transfer of lithium ions and electrons along the grain boundaries, as well as their subsequent diffusion into the bulk of each particle, are required to ensure effective charging. Diffusion along the grain boundaries generally proceeds faster due to the high defect concentration [20]. The length of grain boundaries is, however, considerably larger than the diffusion path length in the bulk of the particles. To enhance the diffusion along the boundaries, the LiFePO_4 particles are coated by carbon [21, 22]. Furthermore, carbon coating prevents the particles growth. A synthesis of LiFePO_4 composites with nanoscale carbon has been reported

[23]. Carbon coating, using polyvinylidene fluoride as the carbon source, with the simultaneous addition of silver have yielded good results [24]. This process provides a highly conducting carbon coating, and partial modification of the LiFePO_4 surface.

It is reasonable to use nanosized LiFePO_4 in order to increase the diffusion in the bulk [13, 25]. Since the conductivity of LiFePO_4 is one-dimensional, it is reasonable to obtain nanoparticles with minimum size along the direction of conduction channels [26]. Formation of such particles can be ensured by using complexing agents. However, there are no advantages of the platelet-shaped nanoparticles with the required orientation and about 15 nm in thickness over isotropic nanoparticles with a mean size of about 40 nm [27].

Since the lithium transfer is determined by ion conductivity firstly [17], heterovalent doping can be the promising solution [28–31]. Information on which sites heterovalent ions are substituted for is quite controversial. Thus, insertion of Mg^{2+} and Cu^{2+} into either iron or lithium sites has been reported by various authors [32–35].

Mössbauer spectroscopy studies demonstrated that divalent cobalt and nickel occupy iron sites in LiFePO_4 with ordered distribution. For example, small amount of Co^{2+} is distributed in such a way that every iron ion contains no more than one cobalt ion in the second coordination sphere [21, 36]. The best results, however, were observed in the case of Ni^{2+} ions doping. A good cycling stability of $\text{Li}_x\text{Fe}^{III}_{1-x}\text{M}^{II}_x\text{PO}_4$ samples at high current densities is of particular importance. It is possible to achieve charge or discharge up to 50 % of the theoretical capacity for such materials in 5 min only (Fig. 1) [36]. Magnesium ions, on the contrary, substitute lithium ions to a great extent, leading to a conductivity and electrochemical capacity decrease [17, 36].

In the case of partial iron substitution with divalent ions, conductivity increase of the oxidized phase is determined by the persistence of lithium ions in the lattice and thus serving as interstitials in $\text{Li}_x\text{Fe}^{III}_{1-x}\text{M}^{II}_x\text{PO}_4$. The reason for this conductivity increase in the reduced phase is, in contrast, not so obvious. Presumably, it can be a result of an ordered distribution of the dopant ions, which favors structurization of lithium transport pathways.

At the same time, simultaneous substitution of iron with two types of cations, which are stable both in divalent and trivalent states, could be even more efficient. The reduced form $\text{Li}_{1-x}\text{Fe}_{1-2x}(\text{M}^{II}\text{M}^{III})_x\text{PO}_4$ should contain a considerable concentration of lithium vacancies. Indeed, such samples demonstrated high capacity and cycling stability, although poorer properties compared to the materials, doped solely with divalent ions [38, 39]. This is mainly due to the faster lithium ion transfer by interstitials [40]. Lithium vacancies formation, in turn, prevents lithium ion transfer into the interstitials.

Even in the case of the successful substitution of a part of iron ions with heterovalent ions, the charge change of dopant ions becomes impossible and results in electrochemical capacity loss at low charge/discharge rates. From this point of view another attractive approach is to substitute iron with ions that could change their valence with the similar potential range. Substitution of iron with manganese ensures full retention of the electrochemical capacity. Capacity of such samples at high rates is also slightly lower, compared

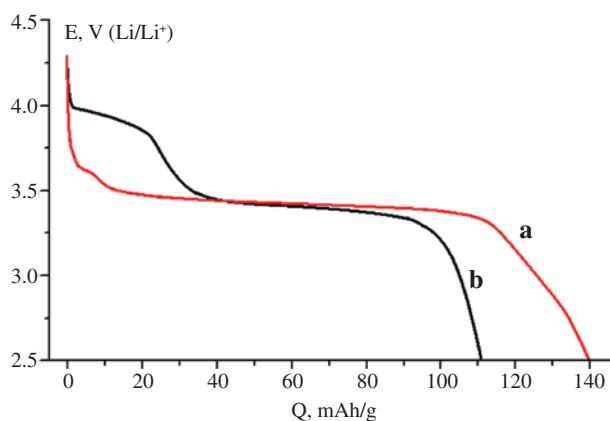


Fig. 1: Discharge curves at 20 mA/g for $\text{LiFe}_{0.9}\text{Mn}_{0.1}\text{PO}_4/\text{C}$ (a) and $\text{LiFe}_{0.7}\text{Mn}_{0.3}\text{PO}_4/\text{C}$ (b) [37].

to the samples doped with cobalt or nickel. Moreover, the second plateau at higher voltage has appeared on charge/discharge curves (Fig. 1). In these materials, manganese, unlike iron, is charged without phase separation according to the solid solution mechanism [37, 41].

Anode materials based on lithium titanate

Much attention has been attracted to lithium titanate – based anode materials. Its composition can be written as $\text{Li}[\text{Li}_{1/3}\text{Ti}_{5/3}]\text{O}_4$; showing that a part of lithium occupies titanium sites, while the lithium itself occupies both octahedral and tetrahedral sites. This compound can intercalate one more lithium ion, converting thereby to $\text{Li}_2[\text{Li}_{1/3}\text{Ti}_{5/3}]\text{O}_4$ ($\text{Li}_7\text{Ti}_5\text{O}_{12}$). Its theoretical electrochemical capacity is 175 mAh/g [42]. In spite of the fact that lithiated and delithiated forms have different structures (spinel and rock-salt type), conversion from the charged to the discharged state results in extremely small changes in the lattice parameter (from 8.3595 to 8.3538 Å) [43, 44]. This provides a high cycling stability of the material, despite the low mutual solubility of the $\text{Li}_{6.93}\text{Ti}_5\text{O}_{12}$ and $\text{Li}_{4.03}\text{Ti}_5\text{O}_{12}$ phases, which coexist during the electrochemical cycle [17].

This material should be used in a nanoscale form because of its low electron and lithium conductivity [13, 45]. Low synthesis temperature, generally used to reduce particle size. A positive effect has been achieved in the case of $\text{Li}_4\text{Ti}_5\text{O}_{12}/\text{C}$ [46–49] or $\text{Li}_4\text{Ti}_5\text{O}_{12}\text{--TiO}_2$ nanocomposites formation [50–53]. In the latter case, properties improvement can be determined by the sorption processes at interfaces, which in their turn results in conductivity increase [54].

Heterovalent doping of $\text{Li}_4\text{Ti}_5\text{O}_{12}$ with various divalent, trivalent and pentavalent cations was performed to enhance its conductivity [55–58]. Although, even when the conductivity of the doped materials increased, their electrochemical capacity decreased. The reason for this is the partial elimination of dopant ions, which substitute titanium, from the electrochemical cycle. At the same time, it enables to increase sample capacity at high current densities [59]. Another feature of such materials appears to be more attractive. During the $\text{Li}_4\text{Ti}_5\text{O}_{12}$ charge only 60 % of titanium ions are reduced to trivalent state. This fact is determined by the limit on the number of cations which can be incorporated in $\text{Li}_7\text{Ti}_5\text{O}_{12}$, which has the NaCl-type structure. A number of attempts of material cycling in an extended potential range were made in order to increase its capacity [60, 61]. However, in these conditions the samples degrade rapidly, especially at high charge/discharge rates. At the same time, cycling stability of gallium-doped sample is markedly higher at such potentials (Fig. 2) [59]. For example, at the current density of 20 mA/g, it is about 235 mAh/g, corresponding to an almost full conversion of titanium into a trivalent state. Even at the current density as high as 1600 mA/g its electrochemical capacity is 118 mAh/g and exceeds that of the undoped sample five times. Furthermore, this material restores initial capacity after returning to the current density of 20 mA/g, showing outstanding cycling stability. The key question is which sites are occupied by the trivalent metal ions. Mössbauer spectroscopy study of lithium

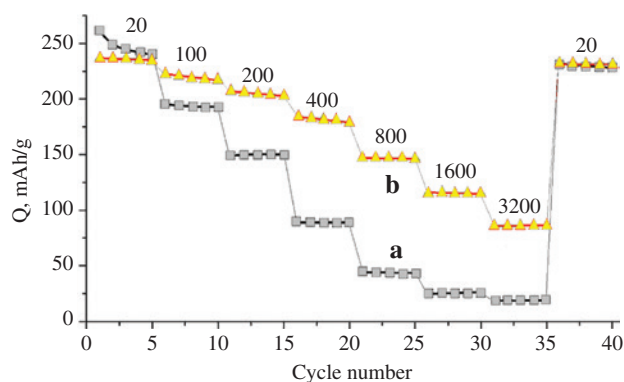


Fig. 2: Discharge capacity curve of $\text{Li}_4\text{Ti}_5\text{O}_{12}$ (a) and $\text{Li}_{4+x-3y}\text{Ti}_{5-x}\text{Ga}_{x+y}\text{O}_{12}$ ($x+y=0.2$) (b) at different current densities. The current density values [mA/g] are shown in the Figure.

titanate with titanium partially substituted with the ^{57}Fe isotope was performed to understand this. It was found that in this case approximately 1/3 of iron ions occupy lithium sites [62]. Meanwhile, according to the Rietveld refinements gallium ions occupy lithium sites predominantly.

A number of efforts have been made to develop alternative anode materials with improved safety, cycling stability, and rate performance. Alternative anode materials with improved safety, cycling stability, and rate performance are being developed at present [63].

Hybrid ion exchange membranes

The main advantage of membranes is associated with their transport properties, determined by the presence of nanoscale pores and channels system within their structure [64]. In ion exchange membranes pores and channels are formed as a result of self-organization processes, during which the hydrophobic chains form the membrane matrix, while the hydrophilic ion exchange groups are grouped in clusters and adsorb water molecules from the contacting solution. High ionic conductivity of the membranes is determined by water solution in these pores and channels with counter-ions formed by functional group dissociation [65–67]. Their mechanical properties are determined defined by the hydrophobic polymer matrix.

Synthesis of hybrid membranes

Since the late 1980s, synthesis and investigation of hybrid membranes, containing inorganic nanoparticles, has been rapidly developing. Firstly, it is due to the prospects of their application in fuel cells [10, 68–75].

In the first works, such membranes were obtained by the casting method with pre-dispersed inorganic nanoparticles [68]. However, it is difficult to ensure efficient particle distribution by using this approach, due to the tendency to agglomeration. A more promising approach is to obtain nanoparticles directly inside the pores of ion exchange membranes. The pores hence act as certain nanoreactors [76], absorbing the initial reagents and limiting the reaction volume. It is important to note that pore walls isolate the formed particles and can reduce the surface tension, ensuring their thermodynamic stability [77]. Owing to the limited size of the nanopores, the diameter of these nanoparticles usually is 2–5 nm (Fig. 3a) [80]. Increasing the number of synthesis cycles and the precursor concentration leads to an increase in nanoparticle size. However, with such a synthesis method, it is not possible to increase the dopant concentration above several volume percent, as well as substantially increase the particle size.

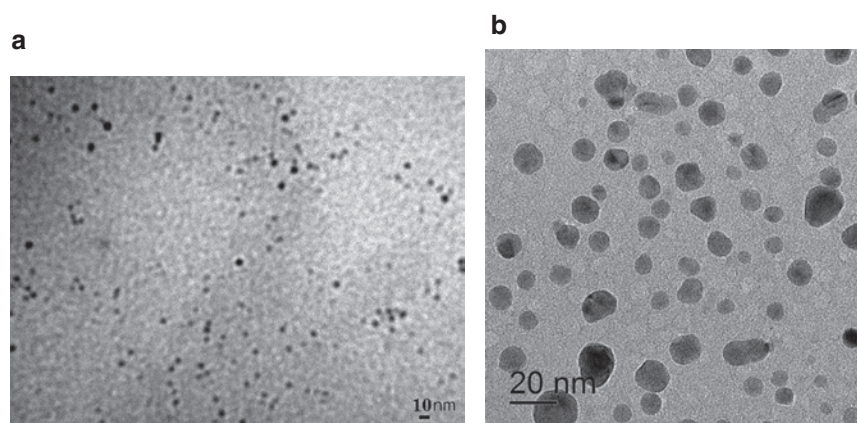


Fig. 3: TEM micrographs of Nafion membranes with incorporated SiO_2 particles, synthesized in-situ (a) [78], or obtained through membrane casting with pre-formed $\text{Cs}_x\text{H}_{3-x}\text{PW}_{12}\text{O}_{40}$ particles (b) [79].

The dopant concentration can be increased by casting the membrane from a solution, containing a precursor for the nanoparticle synthesis. Subsequently, the membrane is treated with a second reagent similar to the above-mentioned approach. There are no restrictions on particle size in this case, and it can become considerably larger (Fig. 3b) [78, 79, 81].

Ionic conductivity of hybrid membranes

In the first works devoted to the synthesis and investigation of hybrid membranes their enhanced ionic conductivity and improved mechanical properties were pointed out. It was the possibility of ionic conductivity increasing that drew close attention of the researchers to hybrid membranes. Hydrated silica, obtained from tetraethylorthosilicate or other organosilicon compounds are the most commonly used dopant for membrane modification [82–84]. Conductivity increase of Nafion/SiO₂ hybrid membranes was mentioned in a number of papers [85–91], whereas its decrease was observed in the others [84, 92, 93]. Discrepancies in the obtained data were most probably determined by the synthesis method of the membranes and the dopant particle size. Increase in conductivity of the hybrid membranes is accompanied by the decrease of their activation energy up to 10–12 kJ/mol [89].

Similar results were obtained for the ion exchange membranes doping with other oxides or salts nanoparticles [94]. In several works this phenomenon was explained by an increase in water uptake. However, there is a number of systems for which ionic conductivity increases, despite a decrease in water uptake [70]. In this regard a model of limited semielasticity of membrane pore walls was suggested which explains this phenomenon [95]. When a nanoparticle is introduced into the membrane, it occupies a part of its volume. Water uptake of membrane is determined by the high propensity of protons to hydration. Since the number of functional groups and protons formed by their dissociation does not change, the degree of hydration should be also maintained on the same level or even get higher in the case of hydrophilic particles. This leads to an increase in volume of pores and channels connected them. It is the increase in the size of the channels that limit the membrane conductivity, which leads to its increase. This assumption is confirmed by the NMR and impedance spectroscopy data for a series of hybrid membranes. The diffusion coefficient of proton-containing groups, which is determined by diffusion in pores, can be both higher and lower for membranes with different dopants, compared to the pristine membrane. Their conductivity, in contrary, being determined by ion transfer in channels, always increases for the doped samples [96].

An improvement of hybrid membrane conductivity at low humidity, reported in a number of papers should be pointed. Conductivity of membranes doped with both silica and heteropolyacids matched that of the pristine membrane at high humidity. At low humidity, the gain in conductivity was considerably higher [97]. As reported previously [80], at 9 % relative humidity the conductivity of hybrid membranes increased by 2.5 orders of magnitude in comparison with initial ones. A substantial improvement of conductivity at low humidity was observed for a Nafion hybrid membrane incorporating by metal–organic frameworks immobilized with phytic (myo-inositol hexaphosphonic) acid [98].

The increase in the ionic conductivity at low humidity is most likely determined by two factors. Presence of the dopant particles inside the pores prevents annihilation of the conduction channels by maintaining the size of the pores. In addition, the electronegative atoms on the dopant surface can contribute to the ion transfer. Their impact is especially important at low water uptake [77].

Hybrid membranes use in fuel cells

Modification of membranes with nanoparticles can result in their selectivity improvement. In the case of cation exchange membranes it can be expressed by the anion transfer numbers. The lower the transfer number, the greater is the selectivity. For example, modification of MF-4SC membranes (a Russian analogue of Nafion membranes) leads to decrease their anion transfer numbers by 2–4 orders of magnitude [99, 100].

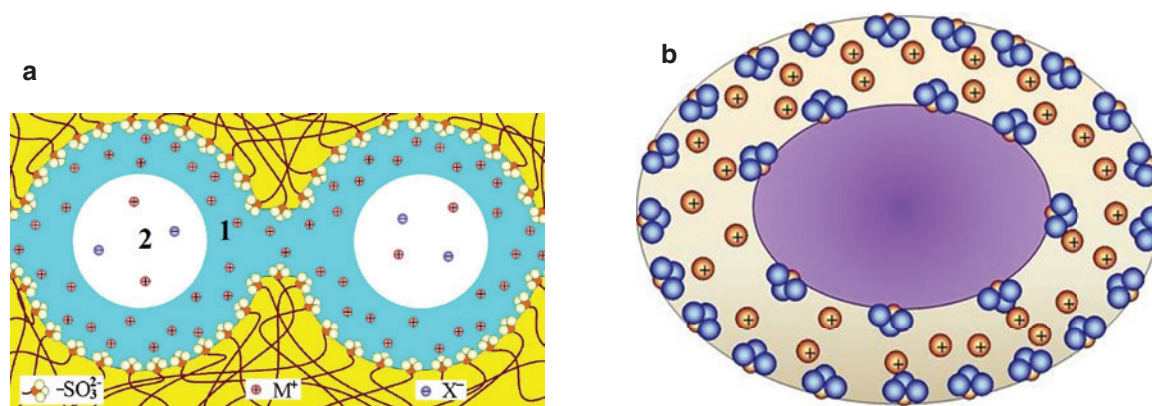


Fig. 4: Schematic distribution of positively and negatively charged ions in the pores of an ion exchange membrane (1 – the Debye layer, 2 – the electroneutral solution) (a) and the formation of the second Debye layer after insertion of a dopant nanoparticle with an acidic surface (b) [77].

Higher selectivity was also achieved by membrane doping with heteropolyacids [79, 80]. Unevenness charge distribution must be the main reason for this. Dissociation of $-SO_3H$ functional groups leads to the negative charge of the membrane pore walls. Meanwhile, due to electrostatic interactions protons are mostly localized in the thin (approx. 1 nm) Debye layer near the pore walls. In the middle of the pore contains an electroneutral solution that contains almost equal amounts of cations and anions in concentrations roughly higher than in the contacting solution (Fig. 4a). So, the total anion concentration, as well as their transfer numbers is much lower, compared to the cations. When an acidic nanoparticle is introduced, its surface also acquires a negative charge, and the particle itself is localized near the center of the pore, displacing a significant part of the electrically neutral solution together with the anions. Concurrently, another Debye layer is formed near the particle surface, facing the first one. This results in decrease of the undesirable anion transfer without hindering the cation transfer within the Debye layer (Fig. 4b) [77]. These effects were recently described quantitatively [101] with the use of microheterogeneous multiphase model. The results of modelling were successfully compared with experimental values of conductivity and diffusion permeability as functions of the nanoparticle volume fraction in a hybrid membrane [102].

At the same time, low-polar molecules of gases and alcohols are also located in the pore centers and forced out during hybrid membrane formation. So an important advantage of the hybrid perfluorinated membranes is the decrease in their permeability to gases and methanol. Low permeability to methanol makes these membranes extremely effective for use in direct methanol fuel cells (DMFC) [103–105]. Sulfonic acid functionalized graphene is explored as a dopant for Nafion membrane. Such hybrid membranes enhanced proton conductivity while restricting the methanol crossover across the membrane. A DMFC with hybrid membrane deliver a peak power density of 118 mW cm^{-2} at a load current density of 450 mA cm^{-2} while operating at 70°C under an ambient pressure. By contrast, operating under identical conditions, a peak power density of 54 mW cm^{-2} at a load current density of 241 mA cm^{-2} is obtained with the pristine recast Nafion membrane [106].

The use of hybrid membranes with incorporated nanoparticles with acidic nature appears to be perspective for the fuel cells using hydrogen. It was shown [97] that the H_2/O_2 fuel cell based on hybrid Nafion–silica membrane doped with phosphotungstic acid, shows the higher current density values than that of pristine membrane. Membranes of this type were also reported to exhibit activity in the catalytic reaction of oxygen reduction [107]. Of particular interest is the fact that a FC based on such membranes shows a lower power density at 100 % relative humidity of the supplied gases (hydrogen, air). As the relative humidity decreases, power density of the cell based on hybrid membrane increases and overruns the performance of the commercial Nafion-212 membranes at 100 % relative humidity (Fig. 5) [108]. Impedance investigation of the membrane-electrode assemblies in the FC operating regime revealed that the reason for this was not only the conductivity increase, but also a decrease in the resistance of the reaction of oxygen reduction at low humidity.

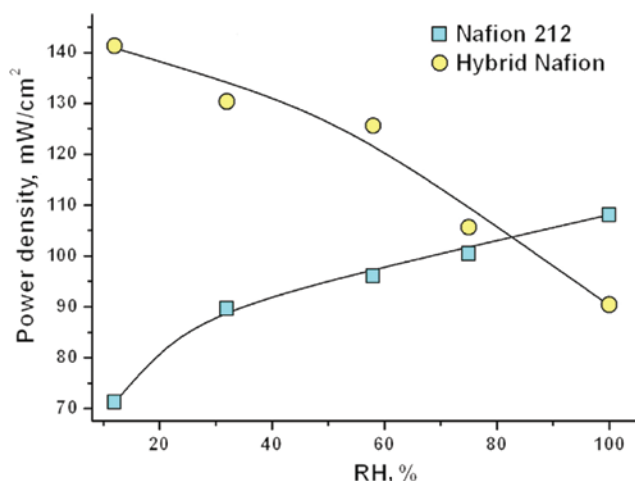


Fig. 5: Maximum power density of the MEAs based on Nafion 212 and hybrid membranes versus relative humidity (RH) of the supplied gases [108].

There are, presumably, large perspectives for application of hybrid membranes based on Nafion and surface-modified nanoparticles [78]. For example, a possibility was demonstrated of transfer selectivity improvement using membranes doped with silica nanoparticles with proton-acceptor properties [109].

Conclusion

Development of modern technologies is largely be related to alternative energy, where a crucial role is played by lithium-ion batteries and fuel cells. Lithium iron phosphate and lithium titanate are promising electrode materials for lithium-ion batteries. Considerable advantages are gained when nanomaterials and carbon composites are used. As for the lithium iron phosphate, the most attractive results were obtained for partial substitution of iron with divalent cations. High electrochemical capacity during cycling in an extended potential range (0.01–3 V) is the most valuable property of lithium titanate partially substituted with trivalent cations. The most promising is the use of these materials in batteries with high power and high charge rate.

As follows from the abovementioned data, incorporation of nanoparticles can lead to a significant improvement of hybrid membrane properties, namely improvement of proton conductivity and gases or methanol permeability of ion exchange membranes. Furthermore, the selectivity of transfer processes is observed in many cases. All this determines possibilities for a wide application of hybrid membranes. It follows from the discussed data that they are widely used in fuel cells design with improved operating characteristics, and in gas separation processes.

Acknowledgments: This work was supported by the Russian Scientific Foundation (project no. 16-13-00127).

References

- [1] V. E. Fortov, O. S. Popel. *Energetika v sovremennoy mire (Russ.)*. p. 167. Intellekt, Dolgoprudny (2011).
- [2] I. A. Stenina, E. Yu. Safronova, A. V. Levchenko, Yu. A. Dobrovolsky, A. B. Yaroslavl'tsev. *Therm. Eng.* **63**, 385 (2016).
- [3] J. E. Girard. *Principles of Environmental Chemistry*, p. 687, Jones & Bartlett Learning, Burlington (2009).
- [4] P. Nema, R. K. Nema, S. Rangnekar. *Renew. Sust. Energ. Rev.* **13**, 2096 (2009).
- [5] P. W. Stackhouse. *Surface Meteorology and Solar Energy*. NASA Langley ASDC. <http://eosweb.larc.nasa.gov/sse/>.
- [6] B. Scrosati, J. Garche. *J. Power Sources* **195**, 2419 (2010).
- [7] M. V. Reddy, G. V. Subba Rao, B. V. R. Chowdari. *Chem. Rev.* **113**, 5364 (2013).

- [8] S. Cleghorn, J. Kolde, W. Liu. "Catalyst coated composite membranes", in *Handbook of Fuel Cells – Fundamentals, Technology and Applications*, W. Vielstich, H. A. Gasteiger, A. Lamm (Eds.), pp. 566–575, John Wiley & Sons, Ltd., Chichester (2003).
- [9] K.-D. Kreuer, S. J. Paddison, E. Spohr, M. Schuster. *Chem. Rev.* **104**, 4637 (2004).
- [10] A. B. Yaroslavl'tsev, Y. A. Dobrovolsky, L. A. Frolova, E. V. Gerasimova, E. A. Sanginov, N. S. Shaglaeva. *Russ. Chem. Rev.* **81**, 191 (2012).
- [11] V. Etacheri, R. Marom, R. Elazari, G. Salitra, D. Aurbach. *Energy Environ. Sci.* **4**, 3243 (2011).
- [12] J. B. Goodenough, K.-S. Park. *J. Am. Chem. Soc.* **135**, 1167 (2013).
- [13] A. B. Yaroslavl'tsev, T. L. Kulova, A. M. Skundin. *Russ. Chem. Rev.* **84**, 826 (2015).
- [14] W.-J. Zhang. *J. Power Sources* **196**, 13 (2011).
- [15] T. Ohzuku, J. Ueda. *J. Electrochem. Soc.* **141**, 2972 (1994).
- [16] B. Xu, D. Qian, Z. Wang, Y. S. Meng. *Mater. Sci. Eng. R Rep.* **73**, 51 (2012).
- [17] D. V. Safronov, S. A. Novikova, A. B. Yaroslavl'tsev, A. M. Skundin. *Inorg. Mat.* **48**, 57 (2012).
- [18] A. K. Padhi, K. S. Nanjundaswamy, J. B. Goodenough. *J. Electrochem. Soc.* **144**, 1188 (1997).
- [19] S. Beninati, L. Damen, M. Mastragostino. *J. Power Sources* **180**, 875 (2008).
- [20] N. F. Uvarov, V. V. Boldyrev. *Russ. Chem. Rev.* **70**, 265 (2001).
- [21] S. A. Novikova, S. A. Yaroslavl'tsev, V. S. Rusakov, T. L. Kulova, A. M. Skundin, A. B. Yaroslavl'tsev. *Mendeleev Commun.* **23**, 251 (2013).
- [22] Q. Fan, L. Lei, X. Xu, G. Yin, Y. Sun. *J. Power Sources* **257**, 65 (2014).
- [23] J. Yang, J. Wang, D. Wang, X. Li, D. Geng, G. Liang, M. Gauthier, R. Li, X. Sun. *J. Power Sources* **208**, 340 (2012).
- [24] D. Gryzlov, S. Novikova, T. Kulova, A. Skundin, A. Yaroslavl'tsev. *Mater. Des.* **104**, 95 (2016).
- [25] D. V. Safronov, I. Y. Pinus, A. B. Yaroslavl'tsev, I. A. Profatilova, V. A. Tarnopolskii, A. M. Skundin. *Inorg. Mater.* **47**, 303 (2011).
- [26] G. X. Wang, S. Bewlay, S. A. Needham, H. K. Liu, R. S. Liu, V. A. Drozd, J.-F. Lee, J. M. Chen. *J. Electrochem. Soc.* **153**, A25 (2006).
- [27] R. R. Kapaev, S. A. Novikova, T. L. Kulova, A. M. Skundin, A. B. Yaroslavl'tsev. *Nanotechnol. Russ.* **11**, 768 (2016).
- [28] K. Hoang, M. D. Johannes. *J. Power Sources* **206**, 274 (2012).
- [29] H. Shu, X. Wang, Q. Wu, B. Hu, X. Yang, Q. Wei, Q. Liang, Y. Bai, M. Zhou, C. Wu, M. Chen, A. Wang, L. Jiang. *J. Power Sources* **237**, 149 (2013).
- [30] H. Gao, L. Jiao, J. Yang, Zh. Qi, Y. Wang, H. Yuan. *Electrochim. Acta* **97**, 143 (2013).
- [31] M.-S. Chen, S.-H. Wu, W. K. Pang. *J. Power Sources* **241**, 690 (2013).
- [32] X. Zhao, D.-H. Baek, J. Manuel, M.-Y. Heo, R. Yang, J. K. Ha, H.-S. Ryu, H.-J. Ahn, K.-W. Kim, K.-K. Cho, J.-H. Ahn. *Mat. Res. Bull.* **47**, 2820 (2012).
- [33] M.-S. Chen, S.-H. Wu, W. K. Pang. *J. Power Sources* **241**, 690 (2013).
- [34] Q. Fan, L. Lei, X. Xu, G. Yin, Y. Sun. *J. Power Sources* **257**, 65 (2014).
- [35] J. Ni, Y. Zhao, J. Chen, L. Gao, L. Lu. *Electrochem. Commun.* **44**, 4 (2014).
- [36] S. Novikova, S. Yaroslavl'tsev, V. Rusakov, T. Kulova, A. Skundin, A. Yaroslavl'tsev. *Electrochim. Acta* **122**, 180 (2014).
- [37] S. Novikova, S. Yaroslavl'tsev, V. Rusakov, A. Chekannikov, T. Kulova, A. Skundin, A. Yaroslavl'tsev. *J. Power Sources* **300**, 444 (2015).
- [38] A. Chekannikov, R. Kapaev, S. Novikova, T. Kulova, A. Skundin, A. Yaroslavl'tsev. *ECS Trans.* **63**, 57 (2014).
- [39] R. Kapaev, S. Novikova, T. Kulova, A. Skundin, A. Yaroslavl'tsev. *J. Solid State Electrochem.* **19**, 2793 (2015).
- [40] A. B. Yaroslavl'tsev. *Russ. Chem. Rev.* **85**, 1255 (2016).
- [41] O. A. Drozhzhin, V. D. Sumanov, O. M. Karakulina, A. M. Abakumov, J. Hadermann, A. N. Baranov, K. J. Stevenson, E. V. Antipov. *Electrochim. Acta* **191**, 149 (2016).
- [42] J. Lu, C. Nan, Q. Peng, Y. Li. *J. Power Sources* **202**, 246 (2012).
- [43] S. Schamer, W. Weppner, P. Schmid-Beurmann. *J. Electrochem. Soc.* **146**, 857 (1999).
- [44] T. Ohzuku, A. Ueda, N. Yamamoto. *J. Electrochem. Soc.* **142**, 1431 (1995).
- [45] T. F. Yi, L. J. Jiang, J. Shu, C. B. Yue, R. S. Zhu, H. B. Qiao. *J. Phys. Chem. Solids* **71**, 1236 (2010).
- [46] W. Fang, X. Q. Cheng, P. J. Zuo, Y. L. Ma, G. Yin. *Electrochim. Acta* **93**, 173 (2013).
- [47] X. Guo, H. F. Xiang, T. P. Zhou, X. K. Ju, Y. C. Wu. *Electrochim. Acta* **130**, 470 (2014).
- [48] I. A. Stenina, A. B. Yaroslavl'tsev, T. L. Kulova, A. M. Skundin. *Russ. J. Inorg. Chem.* **60**, 1380 (2015).
- [49] I. A. Stenina, A. B. Yaroslavl'tsev, S. S. Bukalov, T. L. Kulova, A. M. Skundin, N. Y. Tabachkova. *Nanotechnol. Russ.* **10**, 865 (2015).
- [50] X. Li, C. Lai, C. W. Xiao, X. P. Gao. *Electrochim. Acta* **56**, 9152 (2011).
- [51] J. Wang, H. Zhao, Q. Yang, Ch. Wang, P. Lv, Q. Xia. *J. Power Sources* **222**, 196 (2013).
- [52] T.-F. Yi, Sh.-Y. Yang, Y.-R. Zhu, Y. Xie, R.-S. Zhu. *Int. J. Hydrogen Energy* **40**, 8571 (2015).
- [53] I. A. Stenina, T. L. Kulova, A. M. Skundin, A. B. Yaroslavl'tsev. *Mat. Res. Bull.* **75**, 178 (2016).
- [54] A. B. Yaroslavl'tsev. *Inorg. Mat.* **48**, 1193 (2012).
- [55] Z. J.-Y. Lin, C.-C. Hsu, H.-P. Ho, S.-H. Wu. *Electrochim. Acta* **87**, 126 (2013).
- [56] W. Wang, H. Wang, S. Wang, Y. Hu, Q. Tian, S. Jiao. *J. Power Sources* **228**, 244 (2013).
- [57] J. S. Park, S.-H. Baek, Y.-I. Jeong, B.-Y. Noh, J. H. Kim. *J. Power Sources* **244**, 527 (2013).
- [58] C. Lin, B. Ding, Y. Xin, F. Cheng, M. O. Lai, L. Lu, H. Zhou. *J. Power Sources* **248**, 1034 (2014).

- [59] T. L. Kulova, Yu. M. Kreshchenova, A. A. Kuz'mina, A. M. Skundin, I. A. Stenina, A. B. Yaroslavl'tsev. *Mendeleev Commun.* **26**, 238 (2016).
- [60] J. Shu. *J. Solid State Electrochem.* **13**, 1535 (2009).
- [61] T.-F. Yi, H. Liu, Y.-R. Zhu, L. J. Jiang, Y. Xie, R.-S. Zhu. *J. Power Sources* **215**, 258 (2012).
- [62] I. A. Stenina, A. N. Sobolev, S. A. Yaroslavl'tsev, V. S. Rusakov, T. L. Kulova, A. M. Skundin, A. B. Yaroslavl'tsev. *Electrochim. Acta* **219**, 524 (2016).
- [63] P. A. Nikiforova, I. A. Stenina, T. L. Kulova, A. M. Skundin, A. B. Yaroslavl'tsev. *Inorg. Mat.* **52**, 1137 (2016).
- [64] V. V. Volkov, B. V. Mchedlishvili, V. I. Roldugin, S. S. Ivanchev, A. B. Yaroslavl'tsev. *Nanotechnol. Russ.* **3**, 656 (2008).
- [65] K. A. Mauritz, R. M. Warren. *Macromolecules* **22**, 1730 (1989).
- [66] A. B. Yaroslavl'tsev, V. V. Nikonenko, V. I. Zabolotsky. *Russ. Chem. Rev.* **72**, 393 (2003).
- [67] K. D. Kreuer, S. Paddison, E. Spohr, M. Schuster. *Chem. Rev.* **104**, 4637 (2004).
- [68] D. J. Jones, J. Roziere. "V. 3: Fuel Cell Technology and Applications", in *Handbook of Fuel Cells – Fundamentals, Technology and Applications*, W. Vielstich, H. A. Gasteiger, A. Lamm (Eds.), p. 447, John Wiley & Sons, Ltd., Chichester (2003).
- [69] T. Xu. *J. Membr. Sci.* **263**, 1 (2005).
- [70] A. B. Yaroslavl'tsev, V. V. Nikonenko. *Nanotechnol. Russ.* **4**, 137 (2009).
- [71] H. Ahmad, S. K. Kamarudin, U. A. Hasran, W. R. W. Daud. *Int. J. Hydrogen Energy* **35**, 2160 (2010).
- [72] S. J. Peighambari, S. Rowshanzamir, M. Amjadi. *Int. J. Hydrogen Energy* **35**, 9349 (2010).
- [73] S. Bose, T. Kuila, T. X. Hien Nguyen, N. H. Kim, K.-T. Lau, J. H. Lee. *Progr. Polym. Sci.* **36**, 813 (2011).
- [74] B. P. Tripathi, V. K. Shahi. *Progr. Polym. Sci.* **36**, 945 (2011).
- [75] A. B. Yaroslavl'tsev, Y. P. Yampolskii. *Mendeleev Commun.* **24**, 319 (2014).
- [76] A. B. Yaroslavl'tsev. *Russ. Chem. Rev.* **78**, 1013 (2009).
- [77] A. B. Yaroslavl'tsev. *Nanotechnol. Russ.* **7**, 437 (2012).
- [78] E. Yu. Safronova, A. B. Yaroslavl'tsev. *Solid State Ion.* **221**, 6 (2012).
- [79] A. K. Osipov, E. Yu. Safronova, A. B. Yaroslavl'tsev. *Petrol. Chem.* **56**, 1023 (2016).
- [80] E. Yu. Safronova, I. A. Stenina, A. B. Yaroslavl'tsev. *Russ. J. Inorg. Chem.* **55**, 13 (2010).
- [81] E. Yu. Safronova, A. B. Yaroslavl'tsev. *Russ. J. Inorg. Chem.* **55**, 1499 (2010).
- [82] S. Ren, G. Sun, C. Li, Z. Liang, Z. Wu, W. Jin, X. Qin, X. Yang. *J. Membr. Sci.* **282**, 450 (2006).
- [83] R. Jiang, H. R. Kunz, J. M. Fenton. *J. Membr. Sci.* **272**, 116 (2006).
- [84] A. D'Epifanio, B. Mecher, E. Fabbri, A. Rainer, E. Traversa, S. Licoccia. *J. Electrochem. Soc.* **154**, B1148 (2007).
- [85] S. K. Young, W. L. Jarrett, K. A. Mauritz. *Polym. Eng. Sci.* **41**, 1529 (2001).
- [86] Y. J. Kim, W. C. Choi, S. I. Woo, W. H. Hong. *J. Membr. Sci.* **238**, 213 (2004).
- [87] R. Gosawali, S. Chirachanchai, H. Manuspiya, E. Traversa. *Catal. Today* **118**, 259 (2006).
- [88] Y. Tominaga, I. C. Hong, S. Asai, M. Sumita. *J. Power Sources* **171**, 530 (2007).
- [89] E. Yu. Voropaeva, I. A. Stenina, A. B. Yaroslavl'tsev. *Russ. J. Inorg. Chem.* **53**, 1677 (2008).
- [90] F. Pereira, K. Vallé, P. Belleville, A. Morin, S. Lambert, C. Sanchez. *Chem. Mater.* **20**, 1710 (2008).
- [91] S. Mulmi, C. H. Park, H. K. Kim, Y. M. Lee. *J. Membr. Sci.* **344**, 288 (2009).
- [92] H. Xu, M. Wu, Y. Liu, V. Mittal. *Fuel Cells Bull.* **12**, 12 (2006).
- [93] R. Jiang, H. R. Kunz, J. M. Fenton. *J. Membr. Sci.* **272**, 116 (2006).
- [94] A. B. Yaroslavl'tsev. *Polym. Sci. Ser. A* **55**, 674 (2013).
- [95] S. A. Novikova, E. Yu. Safronova, A. A. Lysova, A. B. Yaroslavl'tsev. *Mendeleev Commun.* **20**, 156 (2010).
- [96] E. Yu. Voropaeva, A. S. Shalimov, I. A. Stenina, A. B. Yaroslavl'tsev, E. A. Sanginov, V. I. Volkov, A. A. Pavlov. *Russ. J. Inorg. Chem.* **53**, 1536 (2008).
- [97] Z.-G. Shao, P. Joghee, I.-M. Hsing. *J. Membr. Sci.* **229**, 43 (2004).
- [98] Z. Li, G. He, B. Zhang, Y. Cao, H. Wu, Z. Jiang, Z. Tiantian. *ACS Appl. Mat. Interfaces* **6**, 9799 (2014).
- [99] A. S. Shalimov, A. I. Perepelkina, I. A. Stenina, A. I. Rebrov, A. B. Yaroslavl'tsev. *Russ. J. Inorg. Chem.* **54**, 356 (2009).
- [100] E. Yu. Safronova, A. S. Shalimov, A. B. Yaroslavl'tsev, V. I. Volkov. *Polym. Sci. Ser. A* **55**, 666 (2013).
- [101] M. Porozhnyy, P. Huguet, M. Cretin, E. Safronova, V. Nikonenko. *Int. J. Hydrogen Energy* **41**, 15605 (2016).
- [102] E. Yu. Safronova, I. A. Prikhno, G. Yu. Yurkov, A. B. Yaroslavl'tsev. *Chem. Eng. Trans.* **43**, 679 (2015).
- [103] W. Xu, T. Lu, C. Liu, W. Xing. *Electrochim. Acta* **50**, 3280 (2005).
- [104] J. Shan, G. Vaivars, H. Luo, R. Mohamed, V. Linkov. *Pure Appl. Chem.* **78**, 1781 (2006).
- [105] C. H. Rhee, Y. Kim, J. S. Lee, H. K. Kim, H. Chang. *J. Power Sources* **159**, 1015 (2016).
- [106] V. Parthiban, S. Akula, S. G. Peera, N. Islam, A. K. Sahu. *Energy Fuels* **30**, 725 (2016).
- [107] E. V. Gerasimova, E. Yu. Safronova, A. A. Volodin, A. E. Ukshe, Yu. A. Dobrovolsky, A. B. Yaroslavl'tsev. *Catal. Today* **193**, 81 (2012).
- [108] E. V. Gerasimova, E. Yu. Safronova, A. E. Ukshe, Yu. A. Dobrovolsky, A. B. Yaroslavl'tsev. *J. Chem. Eng.* **305**, 121 (2016).
- [109] A. G. Mikheev, E. Yu. Safronova, G. Yu. Yurkov, A. B. Yaroslavl'tsev. *Mendeleev Commun.* **23**, 172 (2013).